Journal of Bionic Engineering (2023) 20:2755–2763
https://doi.org/10.1007/s42235-023-00401-6

RESEARCH ARTICLE

High Performance Soft Electrochemical Actuators Based on Hierarchical Conductive Polymer Ionogels

Hongwei Hu[1,2] · Shengtao Zhang[2] · Yan Li[3] · Xinghao Hu[2] · Lin Xu[2] · Aixin Feng[1,6] · Guanggui Cheng[2] · Jianning Ding[4,5]

Received: 21 February 2023 / Revised: 17 May 2023 / Accepted: 18 May 2023 / Published online: 4 August 2023

Abstract

Electrochemical actuators based on conductive polymers are emerging as a strong competitive in the field of soft actuators because of their intrinsically conformable/elastic nature, low cost, low operating voltage and air-working ability. Recent development has shown that adding electroactive materials, such as CNT and graphene, can improve their actuation performance. Despite the complex material systems used, their output strains (one of the key factors) are generally lower than 1%, which limited further applications of them in multiple scenarios. Here, we report soft electrochemical actuators based on conductive polymer ionogels by embedding polyaniline particles between the PEDOT:PSS nanosheets. Results show that such a hierarchical structure not only leads to a high conductivity (1250 S/cm) but also improved electrochemical activities. At a low operating voltage of 1 V, the maximum strain of these soft actuators reaches an exceptional value of 1.5%, with a high blocking force of 1.3 mN. Using these high-performance electrochemical actuators, we demonstrate soft grippers for manipulating object and a bionic flower stimulated by an electrical signal. This work sets an important step towards enabling the enhanced performance of electrochemical actuators based on conductive polymers with designed microstructures.

Keywords Conductive polymer · Soft actuator · Polyaniline · PEDOT:PSS · Bioinspired actuator

1 Introduction

Soft robotics made from high-compliance materials are ideal candidates for applications at the interface of machines and biological systems [1, 2]. The core constituents of soft robotics are soft actuators that exhibit high compliance, distributed actuation and can perform complex motion [3–6]. Owing to their lightweight, compactness and bioinspired motion, these soft actuators are promising for a variety of innovative applications [7–10]. Among the various types of soft actuators, electrochemical actuators driven by reversible ion intercalation in porous electrodes have attracted wide attention because of their low operating voltage (< 5 V), lightweight, large deformation and air working stability [11, 12]. Recent development of conductive polymer-based electrochemical actuators promises a low-cost, easy processing and even lower voltage (< 1 V) driven alternative, and they hold the potential to achieve large strain attributed to their intrinsically high conductivity and high Faraday-type capacitance [11–15].

Poly(3,4-ethylenedioxythiophene)-poly(styrenesulfonate) (PEDOT:PSS), polyaniline (PANI) and polypyrrole are the

✉ Aixin Feng
aixfeng@126.com

✉ Guanggui Cheng
ggcheng@ujs.edu.cn

✉ Jianning Ding
dingjn@ujs.edu.cn

1 Zhejiang Provincial Key Laboratory of Laser Processing Robotics, College of Mechanical and Electrical Engineering, Wenzhou University, Wenzhou 325035, China

2 Institute of Intelligent Flexible Mechatronics, Jiangsu University, Zhenjiang 212013, China

3 School of Mechanical Engineering, Jiangsu University of Science and Technology, Zhenjiang 212100, China

4 School of Mechanical Engineering, Yangzhou University, Yangzhou 225127, China

5 Jiangsu Collaborative Innovation Center of Photovoltaic Science and Engineering, Changzhou University, Changzhou 213164, China

6 Ruian Graduate School of Wenzhou University, Ruian 325207, Zhejiang, China

three commonly used conductive polymers in electrochemical devices [16, 17]. To improve the performance of air-working actuators of these conductive polymers, a lot of efforts have been devoted to develop a hybrid material system combining them with other functional materials, such as CNT, graphene and two-dimensional materials, thereby increasing the electrochemical activities [18–22]. In these hybrid actuators, the actuation is mainly contributed by the guest material, while the conductive polymer is used as a conductive binder to form an elastic network electrode.

Achieving large strain is challenging for pure conductive polymers due to the stringent requirements for high conductivity and high electrochemical activity simultaneously. For example, PEDOT:PSS was used as flexible/strechable electrodes due to its achievable high conductivity ($10^2 \sim 10^3$ S/cm), but its electrochemical activity was low [17, 23–25]. While PANIs with high electrochemical capacitance are extensively studied in electrochemical storage devices, additional conductive fillers are required to increase their inherently low conductivity [16, 26]. In addition to this challenge, the microstructure of conductive polymers that control kinetic ion diffusion, charge storage, and overall electrochemical activity has not been well studied.

To overcome the above limitations, here we report a conductive polymer composite electrode by embedding PANI particles between the PEDOT:PSS nanosheets, forming a hierarchical structure. By tailoring the ratio of these two materials, high conductivity (1250 S/cm) in combination with improved electrochemical activities are achieved. Soft electrochemical actuators based on these electrodes show a large strain of 1.5% at a low operating voltage of 1 V, exceeding the previous values reported for conductive polymer-based actuators. Finally, we show the operational feasibility of our actuators as soft grippers to manipulate objects and electrically controlled bionic flowers. This work sets an important step towards enabling the enhanced performance of electrochemical actuators based on conductive polymers with designed microstructures, paving the way for their future applications.

2 Experimental Section

2.1 Materials

Ionic liquids including 1-butyl-3-methylimidazolium tosylate (BMImOTs, 99%) and 1-Ethyl-3-Methylimidazolium Bis(Trifluoromethylsulfonyl)Imide (EMIMTFSI, 99%) were purchased from Lanzhou Greenchem ILs. BMImOTs was used as an additive for the PEDOT:PSS solution to promote the mechanical property of its thin film. EMIMTFSI was used to prepare the ionogel and gel electrolyte for the actuators. PEDOT:PSS aqueous solution (solid content 1.0–1.3 wt%, PEDOT to PSS ratio is 1:2.5, conductivity > 800 S/cm) was purchased from Shanghai Ouyi Organic Optoelectronic Materials; Ammonium persulfate (APS) and aniline was purchased from Macklin Biochemical.

2.2 Synthesis of PANI Microspheres

The preparation process of PANI microspheres is as follows: 0.4 mL aniline monomer and 11.4 g ammonium persulfate (APS) was dissolved in 10 mL 5 M sulfuric acid solution separately forming solution A and solution B. The two solutions were stored at − 18 °C over 3 h. Then the two solutions were mixed quickly and after shaking for 1 min, the solution was put back to − 18 °C for 12 h. The product was filtered and washed with DI water and dried naturally at room temperature.

2.3 Preparation of Electrode Layers

PEDOT:PSS electrode was prepared by casting method. BMImOTs (5 wt% of the solid content) was added into the PEDOT:PSS solution to promote the separation of PEDOT and PSS chains, thereby improving the film quality. PANI powder of different mass ratios from 2 to 14% was added to the above solution. After stirring for 1 h, and ultrasonic treatment for 15 min, the solution was poured into a Teflon mold and let stand in an ambien environment for 24 h. It was then transferred to an electric oven treated at 60 °C for 2 h and 150 °C for 30 min. After cooling to room temperature, the film was peeled off and immersed in ethanol and DI water subsequently. The ionogel was prepared by immersing the swelled film in ionic liquid and placed at 80 °C for 4 h. The film was then taken out and further dried in a vacuum oven for 8 h.

2.4 Characterization

The electronic conductivity of the films was tested using a four-point probe station (HPS2523). Strain–stress curve was performed on a Mechanical tester (QT-6203S). Cross-sectional SEM images were taken on a JEOL 7800F. XRD was recorded on Bruker D8 Advance. Raman spectra were taken on PLUS Raman microscope (DXR). Electro-chemo-mechanical test was performed using an electrochemical workstation (Gamry 3000) coupled with a laser displacement meter (Panasonic HG-C1050).

2.5 Fabrication and Measurement of Actuators

Two ionogel electrode films were laminated on a cellulose membrane film that was pre-soaked by the ionic liquid. They were then pressed together using two glass slides and placed at 60 °C for 20 min. Afterwards, the trilayer was

carefully peeled off from the glass slides. All the actuators were cut into long strips with 4 mm width and 20 mm length.

The performance of the actuators was measured using a dual channel sourcemeter (Keithley 2602B) for the input power and a laser displacement meter to record the displacement. One end of the actuator was fixed by a Kelvin clamp with two platinum plates on the contact area and the displacement of the free end was recorded by a laser displacement meter. The strain (ε) of the actuator can be calculated by the following equation:

$$\varepsilon = \frac{2d\delta}{(L^2 + \delta^2)} \quad (1)$$

where δ is the tip displacement, d and L are the thickness and and length of the beam, respectively [27]. Blocking force of the actuators was tested using a microforce sensor (FUTEK, NC850) with the testing probe directed against the tip of the actuator.

3 Results and Discussion

The conducting polymer ionogel film was prepared from PEDOT:PSS dispersion containing PANI particles, as illustrated in Fig. 1. The mean particle size of PANI is around 10 µm, as shown in Supplementary Fig. S1. Such a small particle size results in stable dispersion in PEDOT:PSS with the aid of a charged PSS chain. The conductive polymer composite film was then obtained by drying the aqueous dispersion and annealing, resulting in PEDOT:PSS film incorporated with PANI particles (denoted as PANI@PP). The dry film was then immersed in water followed by ionic liquid exchange. This PANI@PP ionogel film was used as electrochemical actuator electrodes by lamination on the two sides of an electrolyte film and the trilayer actuator was then formed by hot-pressing. A cross-sectional SEM image of the actuator is shown in the supplementary information (Fig. S2).

Figure 2 shows the cross-sectional SEM images of PEDOT:PSS film (a) and PANI@PP film (b). The slow

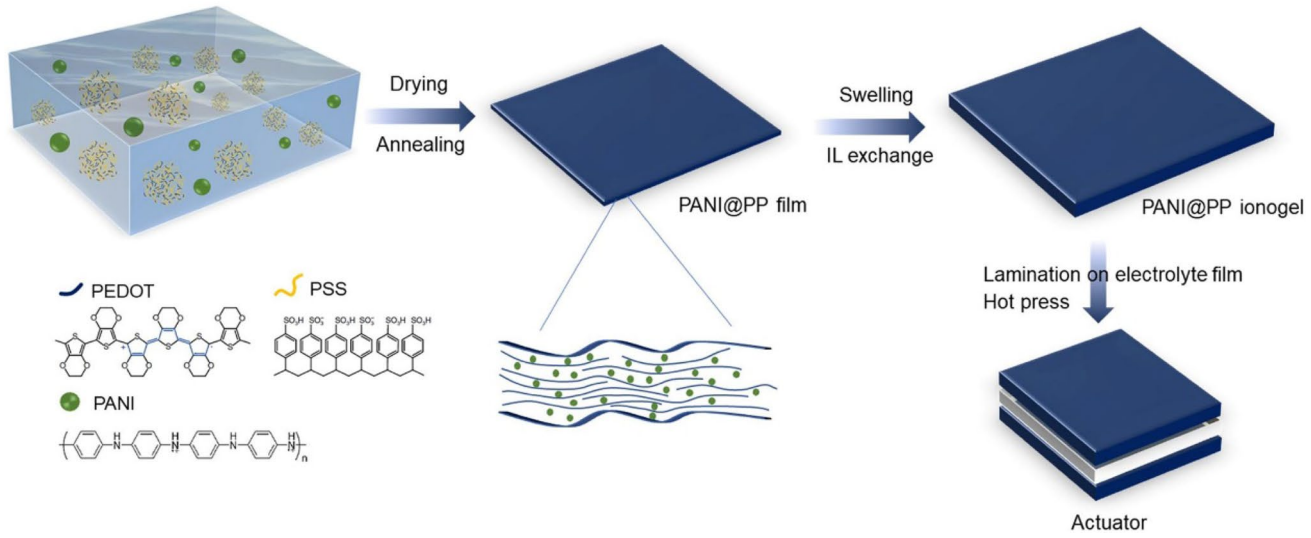

Fig. 1 Schematic illustration of the preparation process of PANI@PP ionogel and actuators

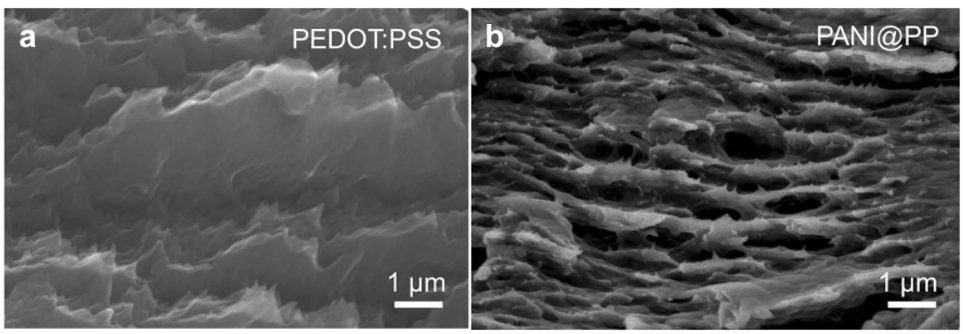

Fig. 2 Cross-sectional SEM images of PEDOT:PSS film (**a**) and PANI@PP film (**b**)

drying of PEDOT:PSS with additives leading to a unique microstructure with compact stacked thin layers, as shown in Fig. 2a. This is due to the slow crystallization of PEDOT chains and PSS chains that gradually separated into thin sheets. As shown in Fig. 2b, the PANI particles were incorporated into the PEDOT:PSS sheets, forming a rough morphology as compared with the nanosheets in pure PEDOT:PSS film. The particle size is much smaller than the pristine PANI, which can be attributed to the redispesion of PANI assisted by the charged PSS chains (Fig. S1). The unique PANI@PP hierarchical structure consisting of conducting PEDOT nanosheets and the high electrochemically active PANI particles facilitates better actuation performance as discussed below.

The conducting polymer plays two roles in electrochemical actuation: the electroactive materials to store charges and current collection layer. Therefore, its electrochemical activity and electronic conductivity are both critical factors in defining the overall actuation performance. The electronic conductivity of the CP films was measured using the four-point probe method. As shown in Fig. 3a, the conductivity of PEDOT:PSS ionogel film reaches 700 S/cm, which is much higher than the dry film without the addition of ionic liquid (~ 50 S/cm). This can be ascribed to the second doping effect from the anions in the ionic liquid [25]. The conductivity was improved dramatically with a small content of PANI in the composite film and the best value of 1250 S/cm was obtained with a 6% weigh ratio of PANI, after which the conductivity starts to drop with a higher amount of PANI presence in the film. The main reason for the increase in conductivity caused by the doping of a small amount of PANI is that PANI particles form a hierarchical structure with the PEDOT:PSS nanosheets, which increased the porosity of the film and facilitated the penetration of ionic liquids. In fact, the ionic liquid uptake ratio of PANI@PP (36.7 wt%) is much larger than that of pure PEDOT:PSS film (16.7 wt%). The ionic liquid in the ionogels can be used as a secondary dopant to improve the conductivity of the PEDOT conductive polymer. However, when the content of PANI in the film is further increased, because the conductivity of PANI is worse than that of PEDOT, the highly conductive network is destroyed by PANI particles, resulting in a decrease in overall conductivity.

To further investigate the reason for the high conductivity of PANI@PP ionogel film, Raman spectra of the dry PEDOT:PSS film, ionic liquid filled PEDOT:PSS ionogel and PANI@PP ionogel were recorded as shown in Fig. 3b. The most prominent peak observed between 1400 and 1500 cm^{-1} is closely associated with the symmetrical $C_\alpha = C_\beta$ stretching vibration of the five-member ring on PEDOT in a polaron state [27]. A redshift was observed for the PEDOT ionogel (peak centered at 1429 cm^{-1}) compared with the dry film (peak centered at 1433 cm^{-1}), which indicates a higher portion of the conductive quinoid structure presenting in the PEDOT chain. This suggests that the ionic liquid as a second dopant has improved the conductivity of the film. The PANI@PP film shows a further redshift to 1427 cm^{-1}, corresponding to its higher conductivity as shown in Fig. 3a. Therefore, the higher ionic liquid uptake ratio for PANI@PP film contributed to a higher doping ratio and subsequently higher conductivity for the ionogel film.

The actuation performance of the conductive polymer-based actuators was tested with a low AC voltage (± 1 V) at a frequency of 0.1 Hz (Fig. 4a). Previous studies have confirmed that the actuation of conductive polymer with large counter ions, such as the PSS used in PEDOT, was driven by the movement of cations [28]. As a result, the negative electrode expands and the positive electrode contracts, causing the three-layer actuator to bend, as shown in the inset images in Fig. 4a. The strain of the actuators, as calculated from the tip displacements, closely correlates to the alternating voltage. The maximum strain differences of these actuators were plotted in Fig. 4b. The pure PEDOT:PSS ionogel-based actuators show a maximum strain of 0.7% at 0.1 Hz of 1 V input voltage and this value was improved to 0.85% with only 2% of PANI in the electrode films. The maximum strain of actuators with 6% of PANI was 1.5%, which is two times higher than the original PEDOT:PSS-based actuators. Further increasing the PANI content leads to a detrimental effect on the output strain. The actuation performance of

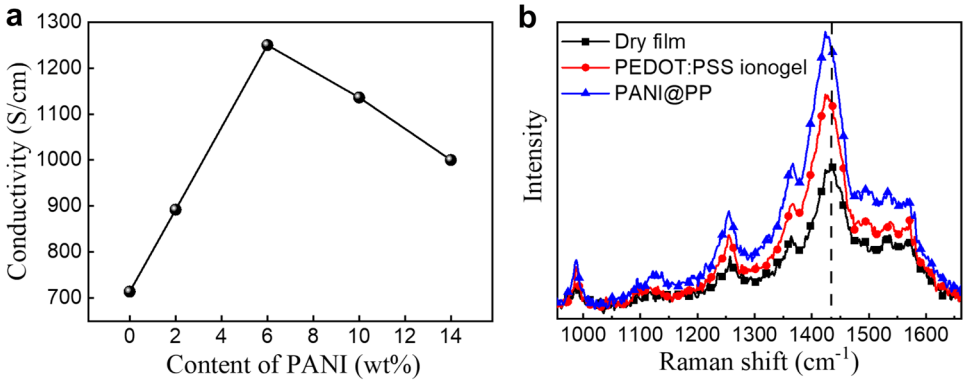

Fig. 3 Conductivity of the ionogel films with different PANI content (**a**) and Raman spectra of the dry film, PEDOT:PSS ionogel and PANI@PP ionogel films (**b**)

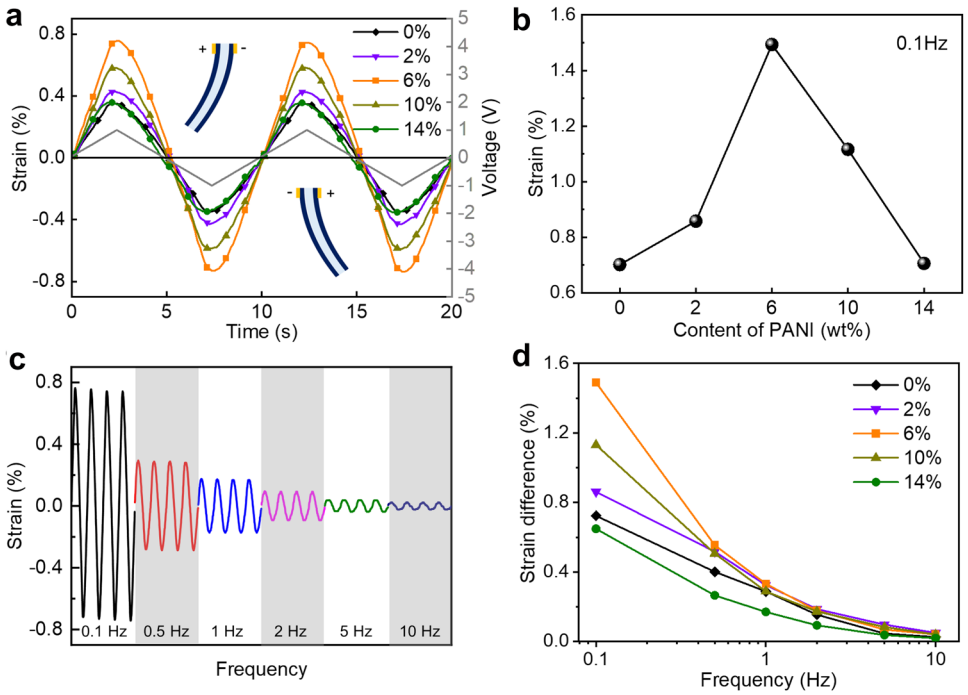

Fig. 4 Actuator performance: **a** the strain of actuators under alternating voltage; **b** the maximum strain of the actuators of varied PANI content at 0.1 Hz 1 V input; **c** the strain of PANI@PP (6 wt% of PANI) under 1 V input from 0.1 to 10 Hz; **d** the frequency-dependent strain of actuators with varied PANI content

different amounts of PANI in the electrodes has a similar trend to their conductivity improvement, indicating that conductivity is one of the key parameters that define actuation performance.

As the electrochemical actuation is caused by the movement of ions in the electrolyte and electrodes under an electrical field, the response time depends on the diffusion of ions, which is a rather slow process. The strain of the actuator with 6 wt% of PANI content operated at a varied frequency from 0.1 to 10 Hz with a fixed amplitude of 1 V are shown in Fig. 4c. As the operating frequency increases, the maximum strain drops sharply, indicating that the slow kinetics of the electrochemical process limit actuation at higher frequencies. This phenomenon presents in all these actuators with varied amounts of PANI (Fig. 4d). The best-performing actuator (with 6 wt% of PANI) shows higher strains at frequencies below 1 Hz and this gap becomes rather small at higher frequencies.

To investigate the actuation mechanism of these electrodes, an electro-chemo-mechanical study was performed by combining the Cyclic voltammetry (CV) test and displacement measurement in a three-electrode configuration. The CV curve shows a pair of redox peaks between − 0.5 V and 0 V versus Ag electrode (Fig. 5a), which can be ascribed to the oxidation and reduction of PEDOT chains. The capacitance can be evaluated from the enclosed area. It is clear that the capacitance is mainly contributed by the oxidation state PEDOT, while the current in the reduced state is significantly reduced. The charge storage on the working electrode was extracted by integrating the current with time. Figure 5b displays the charge storage and tip displacement in 4 cycles of the CV test. These two curves show an almost linear correlation, revealing that the actuation of the electrode was driven by the insertion and desertion of free ions. While the voltage scans toward the negative side, charge stored on the electrode decreases. To maintain an electrostatic balance, additional cations diffused into the electrode and caused volume expansion (corresponding to a positive strain value); On the contrary, when the voltage scans toward the positive side, charge storage increases and these cations were ejected, therefore, caused volume shrinkage.

On the CV curve of PANI@PP electrode, an additional oxidative peak appears on the right side of the PEDOT oxidation peak (Fig. 5c). By using a slow scan rate of 2 mV/s (Fig. S3), this pair of redox peaks was resolved at 0.2 V and − 0.1 V vs. Ag, which belong to the PANI chain. Compared with pure PEDOT:PSS electrodes (27 mF/cm^2), the capacitance is increased to 30 mF/cm^2, which is due to the higher electrochemical activity of PANI. Similar to the PEDOT:PSS electrode, the strain of PANI@PP varies as the charge storage change during the sweeping cycles (Fig. 5d). The strain-to-charge ratio for PANI@PP resulted in 0.7/C, which is higher than the pure PEDOT electrode (0.56/C), suggesting the PANI@PP electrode is more effective in generating volume change per charge.

We further tested the electrochemical performance of the actuators. Figure 6a shows the CV curves obtained at 400 mV/s, corresponding to the devices operated at 0.1 Hz. These scan curves are approximately rectangular, indicating that these actuators resemble double-layer supercapacitors.

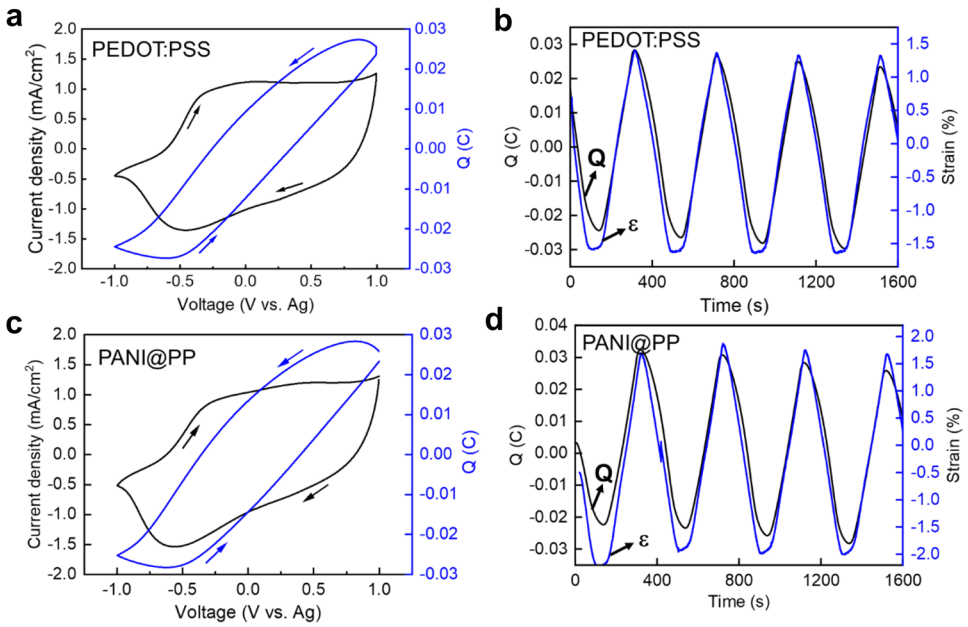

Fig. 5 Electro-chemo-mechanical test of the conductive polymer films in a three-electrode configuration: the CV test (**a**, **c**) and stored charge-strain curves (**b**, **d**)

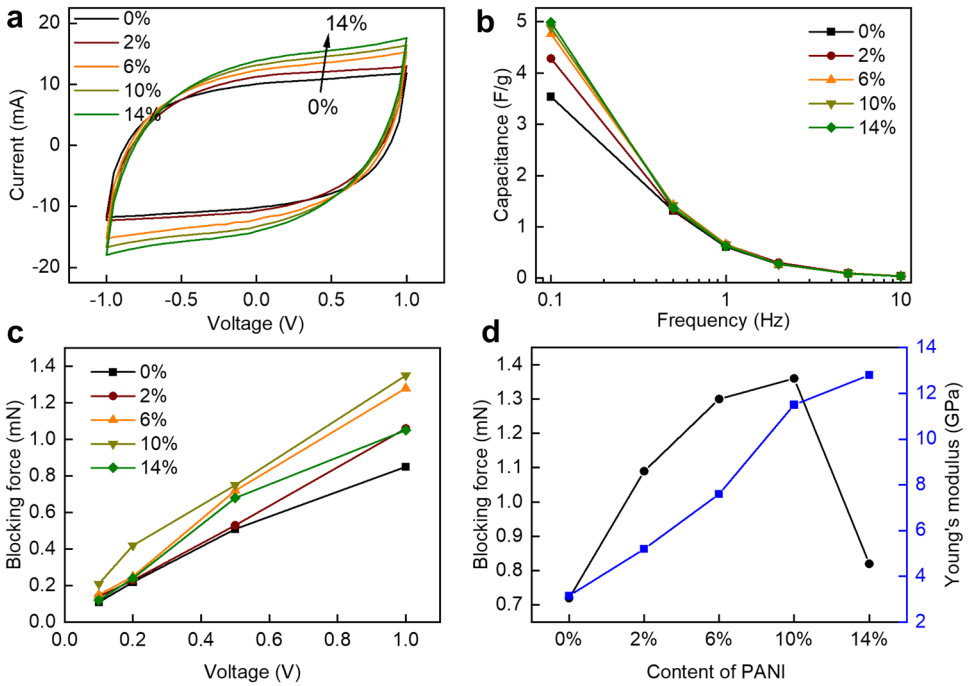

Fig. 6 CV test of the actuators with varied PANI content (**a**); the specific capacitance of the actuators at various frequencies (**b**); the blocking force of the actuators (**c**) and the trend of blocking force and Young's modulus of the electrodes (**d**)

When the amount of PANI in the electrode increases, the current density of the CV scan increases as well as the capacitance. This is due to the higher electrochemical activity of PANI than PEDOT:PSS. Figure 6b displays the capacitance at different scan rate (working frequency), derived from the CV scans. The capacitance of pure PEDOT:PSS-based actuator, tested at 0.1 Hz, reaches 3.5 F/g and this value increased to 4.2 F/g and 4.8 F/g for PANI content of 2% and 6%, respectively. The increment goes down when more amount of PANI added in the electrode. By increasing the scanning frequency, all these values drop sharply and converges to only 0.03 F/g at 10 Hz. This is due to the slow kinetics of electrochemical processes governed by the diffusion of ions.

Figure 6c shows the blocking force of these actuators at given voltages from 0.1 to 1 V. It can be seen that the blocking force is almost linearly related to the applied voltage. The blocking forces at 1 V of the devices with PANI addition were plotted in Fig. 6d. By increasing the content of PANI, the blocking forces increases substantially from 0.71 mN

for pure PEDOT:PSS devices to 1.35 mN with 10 wt% of PANI. This can be explained by the improvement of Young's Modulus of the corresponding electrodes. Although the Young's Modulus of PANI content of 14% is higher, both the conductivity and output strain were affected that resulted in a low blocking force of 0.81 mN. This suggests that the mechanical and electrochemical properties of these conductive polymer composites need to be further optimized to enhance both strain and force.

The practical applications of soft actuators not only require large strain and force but also high working stability. Figure 7a shows the typical cycling test of the PANI@PP-based actuator operated at 1 V and 0.4 Hz for more than 5000 cycles. The actuation performance was well maintained after these cycling, indicating the high durability of these devices. This can be attributed to the high air stability and electrochemical stability of the PANI@PP electrodes.

The conducting polymer-based soft actuators have been investigated for decades and improving their performance has long pursued for further applications. Figure 7b plotted the strains of conducting polymer-based actuators that using ionic liquid as an electrolyte, which is the most promising choice considering their air working stability. Our work on PANI@PP actuators shows higher strain than these reported PANI fiber or yarn-based actuators and the PEDOT actuators enhanced by various electroactive materials, such as MXene and carbon nanotubes (Supplementary Table S1) [19, 20, 29–38].

To verify the potential applications of our conductive polymer actuator, we fabricated a prototype soft gripper using two actuators to manipulate soft objects (Fig. 8a). These intrinsically flexible grippers combined with their infinite degree of freedom actuation make the gripping of irregular or curved surface objects easier than the rigid motor-driven grippers. We further fabricated a bionic flower that can be controlled to bloom and close by electrical signals (Fig. 8b and supplementary video). These examples demonstrate the potential of these conductive polymer-based actuators in multiple scenarios, while following work on the optimization of the fabrication process to achieve miniature devices, or by stacking multiple layers to achieve higher strength will further expand their applications.

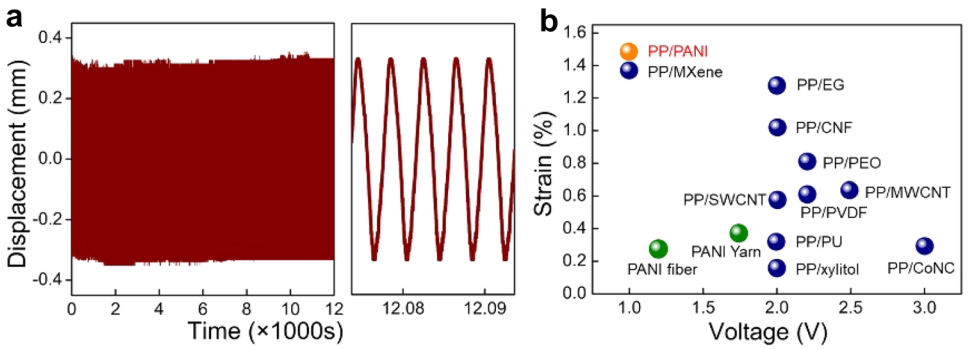

Fig. 7 Stability test (**a**) and a comparison of the actuator performance with reported values (**b**) [19, 20, 29–38]

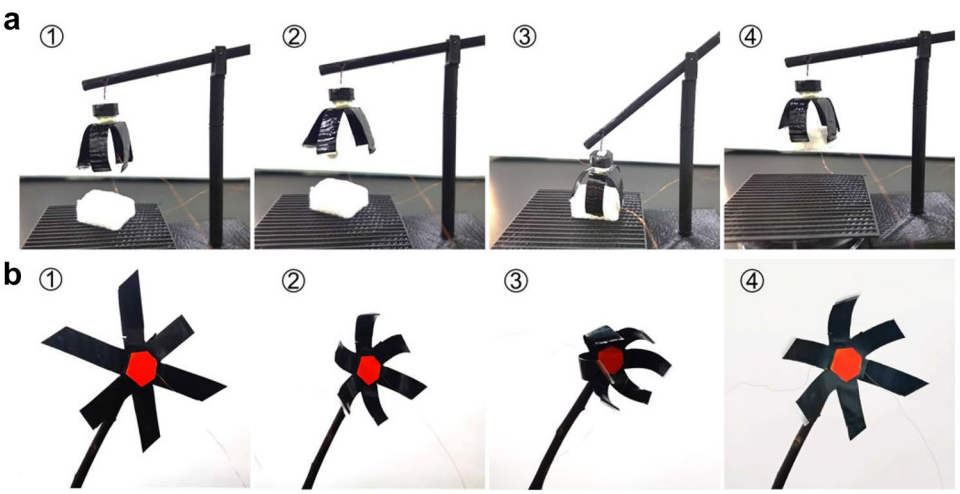

Fig. 8 Demonstration of the soft actuators as soft grippers for manipulating objects (**a**) and bionic flower (**b**)

4 Conclusions

In this work, we have developed conductive polymer ionogel electrodes by embedding PANI particles between the PEDOT:PSS nanosheets to improve the performance of soft electrochemical actuators. The electronic conductivity of these electrodes was improved up to 1250 S/cm due to a high ionic liquid uptake ratio, in combined with an enhanced electrochemical activities. Soft electrochemical actuators using these conductive polymer ionogel electrodes exhibit high performance including a record large strain of 1.5% and a high blocking force of 1.3 mN. The actuation mechanism was further investigated by an electro-chemo-mechanical study, which revealed that the actuation was mainly induced by the insertion and desertion of cations. These results suggest that optimizing the structure and morphology of actuator electrodes is significant to achieve high performance, providing guidance for the future material design for outstanding soft actuators meeting the demand of real-world applications. We have demonstrated soft grippers for manipulating objects and a bionic flower stimulated by an electrical signal. Further research will be conducted to explore more bionic applications based on these soft actuators with larger strain and higher response frequency.

Supplementary Information The online version contains supplementary material available at https://doi.org/10.1007/s42235-023-00401-6.

Acknowledgements This work was supported by China Postdoctoral Science Foundation (2022M711372), Postdoctoral Research Program of Jiangsu Province (2021K544C) and the General Program of Natural Science Foundation for Higher Education in Jiangsu Province (21KJB510004); G. Cheng acknowledges the support from young & middle-aged academic leaders of Jiangsu Blue Project and Jiangsu 333 talent fund; L. Xu acknowledges the support from National Natural Science Foundation of China (NSFC No.51905222) and Natural Science Foundation of Jiangsu Province (Grant No. BK20211068). This work was also supported by International Science and Technology Cooperation Project in Zhenjiang City (Grant No: GJ2020009)

Author Contributions HH: Conceptualization, investigation, data curation, formal analysis, writing—original draft. SZ: Methodology, formal analysis. YL: Characterization, data collection. XH: Investigation, data curation, formal analysis. LX: Investigation, data curation, formal analysis. AF: Conceptualization, investigation, project administration, funding acquisition. GC: Supervision, writing—review and editing. JD: Conceptualization, supervision.

Data Availability The datasets generated during the current study are available from the corresponding author on reasonable request.

Declarations

Conflict of interest The authors declare that they have no known competing financial interests or personal relationships that could have appeared to influence the work reported in this paper.

References

1. Majidi, C. (2014). Soft robotics: A perspective-current trends and prospects for the future. *Soft Robotics, 1*, 5–11. https://doi.org/10.1089/soro.2013.0001
2. Lee, C., Kim, M., Kim, Y. J., Hong, N., Ryu, S., Kim, H. J., & Kim, S. (2017). Soft robot review. *International Journal of Control Automation and Systems, 15*, 3–15. https://doi.org/10.1007/s12555-016-0462-3
3. Li, M., Pal, A., Aghakhani, A., Pena-Francesch, A., & Sitti, M. (2022). Soft actuators for real-world applications. *Nature Reviews Materials, 7*, 235–249. https://doi.org/10.1038/s41578-021-00389-7
4. Miriyev, A., Stack, K., & Lipson, H. (2017). Soft material for soft actuators. *Nature Communications, 8*, 596. https://doi.org/10.1038/s41467-017-00685-3
5. Kim, J., Kim, J. W., Kim, H. C., Zhai, L. D., Ko, H. U., & Muthoka, R. M. (2019). Review of soft actuator materials. *International Journal of Precision Engineering and Manufacturing, 20*, 2221–2241. https://doi.org/10.1007/s12541-019-00255-1
6. Namdar Ghalati, M. H., Akbari, S., Ghafarirad, H., & Zareinejad, M. (2023). Behavior analysis of biomimetic soft bending actuators in free motion and contact. *Journal of Bionic Engineering, 20*, 967–981. https://doi.org/10.1007/s42235-022-00322-w
7. Mirfakhrai, T., Madden, J. D. W., & Baughman, R. H. (2007). Polymer artificial muscles. *Materials Today, 10*, 30–38. https://doi.org/10.1016/S1369-7021(07)70048-2
8. Baughman, R. H. (1996). Conducting polymer artificial muscles. *Synthetic Metals, 78*, 339–353. https://doi.org/10.1016/0379-6779(96)80158-5
9. Mirvakili, S. M., & Hunter, I. W. (2018). Artificial muscles: Mechanisms, applications, and challenges. *Advanced Materials, 30*, 1704407. https://doi.org/10.1002/adma.201704407
10. Wang, J. X., Gao, D. C., & Lee, P. S. (2021). Recent progress in artificial muscles for interactive soft robotics. *Advanced Materials, 33*, 2003088. https://doi.org/10.1002/adma.202003088
11. Kim, O., Kim, S. J., & Park, M. J. (2018). Low-voltage-driven soft actuators. *Chemical Communications, 54*, 4895–4904. https://doi.org/10.1039/c8cc01670d
12. He, Q. S., Yin, G. X., Vokoun, D., Shen, Q., Lu, J., Liu, X. F., Xu, X. R., Yu, M., & Dai, Z. D. (2022). Review on improvement, modeling, and application of ionic polymer metal composite artificial muscle. *Journal of Bionic Engineering, 19*, 279–298. https://doi.org/10.1007/s42235-022-00153-9
13. Baughman, R. H., Shacklette, L. W., Elsenbaumer, R. L., Plichta, E., Becht, C. Conducting polymer electromechanical actuators. In: Brédas, J. L., Chance, R. R. Conjugated polymeric materials: Opportunities in electronics, optoelectronics, and molecular electronics. Springer Netherlands, pp 559–582 (1990).
14. Park, J. M., Kim, S. J., Jang, J. H., Wang, Z. J., Kim, P. G., Yoon, D. J., Kim, J., Hansen, G., & Devries, K. L. (2008). Actuation of electrochemical, electro-magnetic, and electro-active actuators for carbon nanofiber and ni nanowire reinforced polymer composites. *Composites Part B-Engineering, 39*, 1161–1169. https://doi.org/10.1016/j.compositesb.2008.03.009
15. Malinauskas, A., Malinauskiene, J., & Ramanavicius, A. (2005). Conducting polymer-based nanostructurized materials: Electrochemical aspects. *Nanotechnology, 16*, R51–R62. https://doi.org/10.1088/0957-4484/16/10/R01
16. Zhang, X., Wang, T. F., Li, S. J., & Shen, X. J. (2021). Electrodeposition polyaniline nanofiber on the PEDOT:PSS-coated sinws for high performance supercapacitors. *Journal of Inorganic and Organometallic Polymers and Materials, 31*, 4260–4271. https://doi.org/10.1007/s10904-021-02036-8

17. Hu, F. Q., Xue, Y., Xu, J. K., & Lu, B. Y. (2019). PEDOT-based conducting polymer actuators. *Front Robot AI, 6*, 114. https://doi.org/10.3389/frobt.2019.00114
18. Park, J., Lee, A., Yim, Y., & Han, E. (2011). Electrical and thermal properties of PEDOT:PSS films doped with carbon nanotubes. *Synthetic Metals, 161*, 523–527. https://doi.org/10.1016/j.synthmet.2011.01.006
19. Terasawa, N., & Asaka, K. (2016). High-performance PEDOT:PSS/single-walled carbon nanotube/ionic liquid actuators combining electrostatic double-layer and faradaic capacitors. *Langmuir, 32*, 7210–7218. https://doi.org/10.1021/acs.langmuir.6b01148
20. Wang, D. X., Lu, C., Zhao, J. J., Han, S., Wu, M. H., & Chen, W. (2017). High energy conversion efficiency conducting polymer actuators based on PEDOT:PSS/mwcnts composite electrode. *RSC Advances, 7*, 31264–31271. https://doi.org/10.1039/c7ra05469f
21. Jia, G. W., Zheng, A., Wang, X., Zhang, L., Li, L., Li, C. X., Zhang, Y., & Cao, L. Y. (2021). Flexible, biocompatible and highly conductive mxene-graphene oxide film for smart actuator and humidity sensor. *Sensors and Actuators B: Chemical, 346*, 130507. https://doi.org/10.1016/j.snb.2021.130507
22. Sachyani, E., Layani, M., Tibi, G., Avidan, T., Degani, A., & Magdassi, S. (2017). Enhanced movement of cnt-based actuators by a three-layered structure with controlled resistivity. *Sensors and Actuators B: Chemical, 252*, 1071–1077. https://doi.org/10.1016/j.snb.2017.06.104
23. Yano, H., Kudo, K., Marumo, K., & Okuzaki, H. (2019). Fully soluble self-doped poly(3,4-ethylenedioxythiophene) with an electrical conductivity greater than 1000 s cm^{-1}. *Science Advances, 5*, eaav9492. https://doi.org/10.1126/sciadv.aav9492
24. Guo, D. J., Wang, L., Wang, X. J., Xiao, Y. A., Wang, C. D., Chen, L. M., & Ding, Y. H. (2020). PEDOT coating enhanced electromechanical performances and prolonged stable working time of ipmc actuator. *Sensors and Actuators B: Chemical, 305*, 127488. https://doi.org/10.1016/j.snb.2019.127488
25. Wang, Y., Zhu, C. X., Pfattner, R., Yan, H. P., Jin, L. H., Chen, S. C., Molina-Lopez, F., Lissel, F., Liu, J., Rabiah, N. I., Chen, Z., Chung, J. W., Linder, C., Toney, M. F., Murmann, B., & Bao, Z. (2017). A highly stretchable, transparent, and conductive polymer. *Science Advances, 3*, e1602076. https://doi.org/10.1126/sciadv.1602076
26. Pal, R., Goyal, S. L., Rawal, I., Gupta, A. K., & Ruchi. (2021). Efficient energy storage performance of electrochemical supercapacitors based on polyaniline/graphene nanocomposite electrodes. *Journal of Physics and Chemistry of Solids, 154*, 110057. https://doi.org/10.1016/j.jpcs.2021.110057
27. Yemata, T. A., Zheng, Y., Kyaw, A. K. K., Wang, X. Z., Song, J., Chin, W. S., & Xu, J. W. (2020). Binary treatment of PDEDOT:PSS films with nitric acid and imidazolium-based ionic liquids to improve the thermoelectric properties. *Materials Advances, 1*, 3233–3242. https://doi.org/10.1039/d0ma00522c
28. Petroffe, G., Beouch, L., Cantin, S., Aubert, P. H., Plesse, C., Dudon, J. P., Vidal, F., & Chevrot, C. (2018). Investigations of ionic liquids on the infrared electroreflective properties of poly(3,4-ethylenedioxythiophene). *Solar Energy Materials and Solar Cells, 177*, 23–31. https://doi.org/10.1016/J.SOLMAT.2017.07.018
29. Umrao, S., Tabassian, R., Kim, J., Nguyen, V., Zhou, Q. T., Nam, S., & Oh, I. K. (2019). Mxene artificial muscles based on ionically cross-linked $Ti_3C_2T_x$ electrode for kinetic soft robotics. *Science Robotics, 4*, eaaw7797. https://doi.org/10.1126/scirobotics.aaw7797
30. Lu, W., Fadeev, A. G., Qi, B., Smela, E., Mattes, B. R., Ding, J., Spinks, G. M., Mazurkiewicz, J., Zhou, D., Wallace, G. G., Macfarlane, D. R., Forsyth, S. A., & Forsyth, M. (2002). Use of ionic liquids for pi-conjugated polymer electrochemical devices. *Science, 297*, 983–987. https://doi.org/10.1126/science.1072651
31. Lu, W., Norris, I. D., & Mattes, B. R. (2005). Electrochemical actuator devices based on polyaniline yarns and ionic liquid electrolytes. *Australian Journal of Chemistry, 58*, 263–269. https://doi.org/10.1071/ch04255
32. Li, Y. C., Tanigawa, R., & Okuzaki, H. (2014). Soft and flexible PEDOT/PSS films for applications to soft actuators. *Smart Materials and Structures, 23*, 074010. https://doi.org/10.1088/0964-1726/23/7/074010
33. Okuzaki, H., Takagi, S., Hishiki, F., & Tanigawa, R. (2014). Ionic liquid/polyurethane/PEDOT:PSS composites for electro-active polymer actuators. *Sensors and Actuators B-Chemical, 194*, 59–63. https://doi.org/10.1016/J.SNB.2013.12.059
34. Terasawa, N., & Asaka, K. (2018). Self-standing cellulose nanofiber/poly(3,4-ethylenedioxythiophene):Poly(4-styrenesulfonate)/ionic liquid actuators with superior performance. *RSC Advances, 8*, 33149–33155. https://doi.org/10.1039/c8ra06981f
35. Terasawa, N., & Asaka, K. (2018). Performance enhancement of PEDOT: Poly(4-styrenesulfonate) actuators by using ethylene glycol. *RSC Advances, 8*, 17732–17738. https://doi.org/10.1039/c8ra02714e
36. Bar-Cohen, Y., Simaite, A., Tondu, B., Mathieu, F., Souéres, P., & Bergaud, C. (2015). Simple casting based fabrication of PEDOT:PSS-PVDF-ionic liquid soft actuators. *Electroactive Polymer Actuators and Devices (EAPAD)*. https://doi.org/10.1117/12.2083936
37. Rohtlaid, K., Nguyen, G. T. M., Soyer, C., Cattan, E., Vidal, F., & Plesse, C. (2019). Poly(3,4-ethylenedioxythiophene):Poly(styrene sulfonate)/polyethylene oxide electrodes with improved electrical and electrochemical properties for soft microactuators and microsensors. *Advanced Electronic Materials, 5*, 1800948. https://doi.org/10.1002/aelm.201800948
38. Lu, F. Z., Chen, T., Xiang, K., & Wang, Y. N. (2020). Ionic electro-active polymer actuator based on cobalt-containing nitrogen-doped carbon/conducting polymer soft electrode. *Polymer Testing, 84*, 106413. https://doi.org/10.1016/j.polymertesting.2020.106413